Bioorganic Chemistry 92 (2019) 103201

Contents lists available at ScienceDirect

Bioorganic Chemistry

journal homepage: www.elsevier.com/locate/bioorg

Ultrasound mediated efficient synthesis of new 4-oxoquinazolin-3(4*H*)-yl) furan-2-carboxamides as potent tyrosinase inhibitors: Mechanistic approach through chemoinformatics and molecular docking studies

Nilam C. Dige[a,1], Prasad G. Mahajan[b,1], Hussain Raza[a], Mubashir Hassan[c], Balasaheb D. Vanjare[b], Hansol Hong[a], Ki Hwan Lee[b], Jalifah latip[d,*], Sung-Yum Seo[a,*]

[a] Department of Biological Sciences, Kongju National University, Gongju, Chungnam 32588, Republic of Korea
[b] Department of Chemistry, Kongju National University, Gongju, Chungnam 32588, Republic of Korea
[c] Institute of Molecular Biology and Biotechnology, The University of Lahore, Defence Road, Lahore 54590, Pakistan
[d] School of Chemical Sciences and Food Technology, Faculty of Science and Technology, Universiti Kebangsaan Malaysia (UKM), 43600 Bangi, Selangor, Malaysia

ARTICLE INFO

Keywords:
Oxoquinazolin-3(4*H*)-yl)furan-2-carboxamides
Ultrasound sonication
Tyrosinase
Lipinski's rule
Drug score
Molecular docking

ABSTRACT

We have carried out the synthesis of new 4-oxoquinazolin-3(4*H*)-yl)furan-2-carboxamide derivatives by the reaction between isatoic anhydride, 2-furoic hydrazide and substituted salicylaldehydes in ethanol: water (5:5 *v/v*) solvent system using *p*-TSA as a catalyst under ultrasound irradiation at room temperature. The structures of newly synthesized compounds were confirmed through spectral techniques such as IR, ^{1}H NMR, ^{13}C NMR, and LCMS. The important features of this protocol include simple and easy workup procedure, reaction carried out at ambient temperature, use of ultrasound and high yield of oxoquinazolin-3(4*H*)-yl)furan-2-carboxamides in short reaction time. The synthesized compounds **4a–4j** were screened against tyrosinase enzyme and all these compounds found to be potent inhibitors with much lower IC_{50} value of 0.028 ± 0.016 to 1.775 ± 0.947 μM than the standard kojic acid (16.832 ± 1.162 μM). The kinetics mechanism for compound **4e** was analyzed by Lineweaver-Burk plots which revealed that compound inhibited tyrosinase non-competitively by forming an enzyme-inhibitor complex. Along with this all the synthesized compounds **(4a–4j)** were scanned for their DPPH free radical scavenging ability. The outputs received through *in vitro* and *in silico* analysis are coherent to the each other with good binding energy values (kcal/mol) posed by synthesized ligands.

1. Introduction

Human Being is mostly exposed to ultraviolet (UV) radiation, which results into generation of reactive oxygen species. Excessive reactive oxygen species leads to induce skin injuries [1–3]. These UV radiations are being absorbed by Melanin to protect skin cells [4]. Therefore, for human health, normal skin pigmentation is very essential [5]. Generally, tyrosinase is highly cooperative in Melanin synthesis. Tyrosinase is also known as polyphenol oxidase and is a copper-containing enzyme that catalyzes several steps in the synthesis of melanin. It is widely distributed in nature including plants, microorganism and animals [6]. It causes browning of vegetables, beverages, fruits and melanogenesis in animals [7]. It catalyzes two distinct reactions of melanin synthesis such as the hydroxylation of a monophenol (monophenolase activity) and the conversion of an *o*-diphenol to the corresponding *o*-quinone (diphenolase activity) [8]. Along with this, tyrosinase have many other functions like detoxification of host plant defensive phenols for symbiotic bacteria [9,10] and synthesis of amino acid based antibiotics [11]. In relation to hyperpigmentation, tyrosinase inhibitors have become increasingly important in medicinal [12] and cosmetic [13] products. Therefore, design and synthesis of tyrosinase inhibitors is demanding and challenging task before the researchers working in medicinal field.

Quinazolinones are one of the most important heterocyclic structures. It is bicyclic compound possessing a pyrimidine system fused at position 5 and 6 with a benzene ring. They are one of the most important groups of heterocycles in medicinal chemistry [14]. They possess diverse biological activities such as antibacterial, antifungal, anticonvulsant, anti-inflammatory, anti-HIV, anticancer and analgesic [15–25]. Many commercialized drugs have quinazolinone moiety in

* Corresponding authors.
E-mail addresses: jalifah@ukm.edu.my (J. latip), dnalove@kongju.ac.kr (S.-Y. Seo).
[1] These authors contributed equally for this research work.

https://doi.org/10.1016/j.bioorg.2019.103201
Received 10 July 2019; Received in revised form 8 August 2019; Accepted 13 August 2019
Available online 13 August 2019

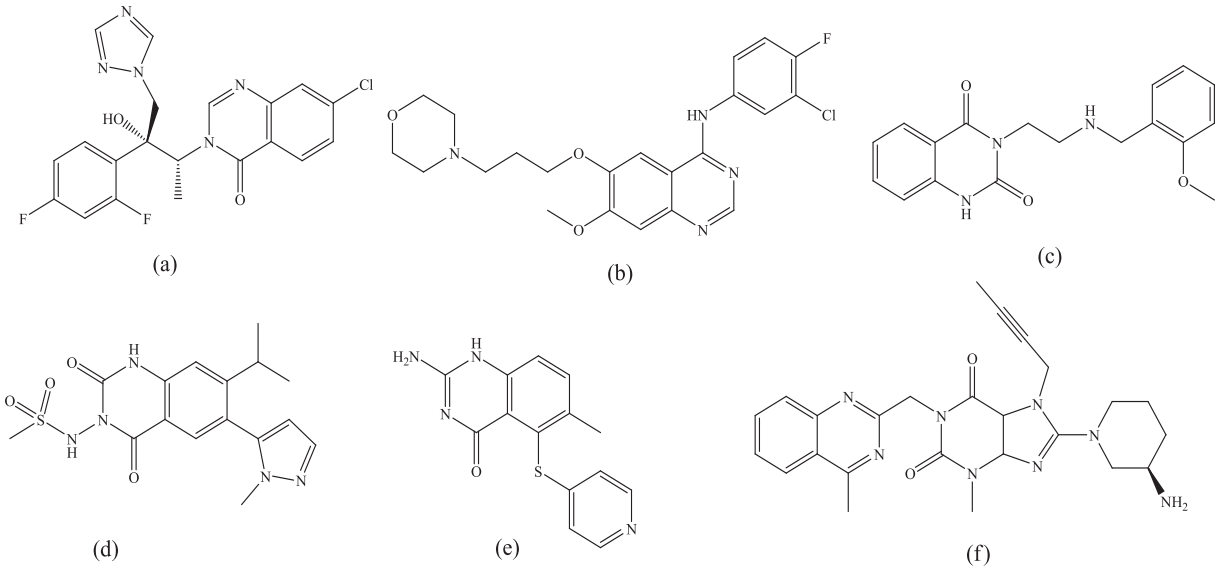

Fig. 1. Examples of commercialized drugs containing quinazolinone moiety in its structure.

their structures, for example Albaconazole (Fig. 1a) used as antifungal agent, Gifitinib(Fig. 1b) used for breast and lung cancer, RH – 34(Fig. 1c) acts as a potent and selective partial agonist for the 5-HT2A serotonin receptor, Selurampanel (Fig. 1d) for the treatment of epilepsy, Nolatrexed (Fig. 1e) is a thymidylate synthase inhibitor and Linagliptin (Fig. 1f) for diabetes mellitus type 2. Recent years also witnessed that the quinazolinone derivatives are important scaffold in the pharmaceutical chemistry [26–31]. Variety of methods are available [32,33] for their synthesis with some drawbacks such as use of toxic and costly catalyst, lower yield of product and use of hazardous solvents. Hence taking these points into consideration, we aimed to design and synthesize new quinazolinone derivatives as potent tyrosinase inhibitors by using economical, safe and swift synthetic approach.

Principally, scientist working in organic chemistry for the development of novel methodologies towards synthesis of heterocyclic compounds follows green chemistry protocols. Ultrasound sonochemistry is one of the significant green chemical methods used to enhance processes through a physical phenomenon known as acoustic cavitation, growth, and collapse of micrometer-sized bubbles when a pressure wave of sufficient intensity propagates through an elastic liquid [34–36]. These protocols have some superiorities such as efficient, fast, clean, eco-friendly, short times, simplicity, controllability and consistent in chemical laboratories as compared to traditional heating methods [37].

Hence, present studies illustrate design and synthesis of new 4-oxoquinazolin-3(4*H*)-yl)furan-2-carboxamides using isatoic anhydride, 2-Furoic hydrazide and various substituted salicylaldehydes under ultrasound sonication. Pleasingly, all reactions proceed well with desired product in good to excellent yield. After successful synthesis and characterization, the synthesized compounds were examined for their tyrosinase activity. All compounds were found to be potent inhibitors against tyrosinase enzyme which was further supported by molecular docking analysis and chemoinformatics properties.

2. Result and discussion

2.1. Chemistry

Initially, we choose a model reaction of isatoic anhydride (1 mmol), 2-Furoic hydrazide (1 mmol) and salicylaldehyde (1 mmol) for the synthesis of 4-oxoquinazolin-3(4*H*)-yl)furan-2-carboxamides (Scheme 1)under ultrasound sonication. As per our early experience [38,39], we try to carry out the reaction at room temperature (RT) in catalyst free condition (**Entry 1,** Table 1). Unfortunately, the reaction did not proceed. Later on, we choose *p*-toluene sulfonic acid (*p*-TSA) as a catalyst in ethanol (**Entry 2,** Table 1). Pleasingly, the reaction proceeds but the yield of product was less than expected. To follow the green chemistry principles, we tried to perform the reaction using water as a green solvent (**Entry 3,** Table 1). Unfortunately, the yield of product was less than the expected. It may be due to the less solubility of reactants in water. Also we tried to perform the reaction in methanol but the time to complete the transformation is more and yield of product was less than ethanol (**Entry 4,** Table 1). Hence, with our earlier experience in mixed solvent system [40,41], we decided to use ethanol: water as mixed solvent system for the model reaction (**Entries 5–13,** Table 1). Remarkably, ethanol: water (5:5 *v/v*) was found to be the best solvent system for the present transformation (**Entry 9,** Table 1).

After successful screening of solvent, we moved towards the screening of catalyst amount (**Entries 14 – 17,** Table 1) in 1:1 ethanol: water solvent system under ultrasonication. From Table 1 we can conclude that 20 mol% of *p*-TSA is sufficient to drive the reaction (**Entry 14,** Table 1). If we use 10 mol% of catalyst then the yield of product was decreased (**Entry 15,** Table 1). Instead of these, when we use more catalytic amount *i.e.* 40 and 50 mol% then no any significant change in yield and time were observed (**Entries 16 and 17,** Table 1). Hence, the ideal reaction conditions for model reaction were followed as 20 mol% of *p*-TSA in Ethanol: water (5:5 *v/v*) solvent under ultrasound sonication.

With these optimized reaction conditions in hand, we have synthesized a library of new 4-oxoquinazolin-3(4*H*)-yl)furan-2-carboxamides using variety of salicylaldehydes with electron donating and withdrawing moiety in its structure (Table 2). All reactions proceed well resulting expected product in good to excellent yield. From Table 2 we can conclude that the time required to complete the transformation for the compound containing electron withdrawing group (4b, 4c, 4d, 4e, 4h) is less as compared to compound having electron donating group in its structure except compound 4j.

After successful synthesis, the characterization of product was done using spectral techniques such as IR, ^{1}H & ^{13}C NMR and LCMS analysis. Pleasingly all the spectral analysis of compounds is in agreement with the proposed structure. Further all the synthesized products (**4a–4j**) have been scanned for their tyrosinase activity. All compounds showed excellent tyrosinase inhibition activity which were further supported by molecular docking and Chemoinformatics studies.

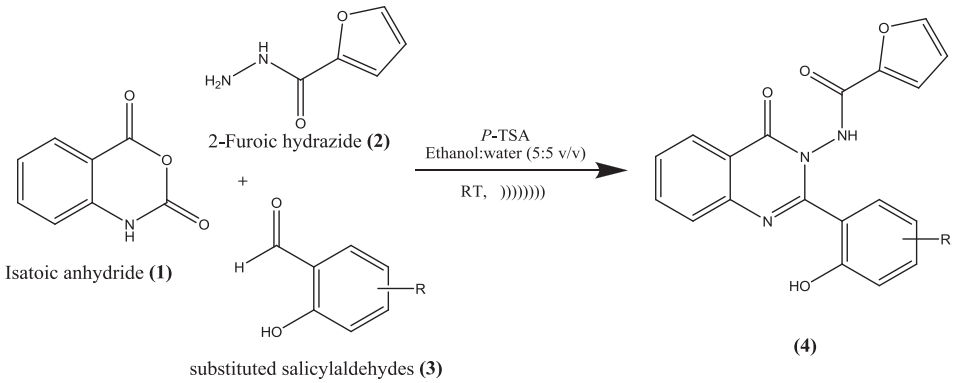

Scheme 1. Synthesis of new 4-oxoquinazolin-3(4*H*)-yl)furan-2-carboxamides.

Table 1
Screening of catalyst and solvent.

Entry	Catalyst	Catalytic amount (mol %)	Solvent	Time (min)	Yield (%)
1	–	–	Ethanol	360	–
2	*p*-TSA	30	Ethanol	120	62
3	*p*-TSA	30	water	180	58
4	*p*-TSA	30	Methanol	180	53
5	*p*-TSA	30	Ethanol: Water (1:9 *v/v*)	105	62
6	*p*-TSA	30	Ethanol: Water (2:8 *v/v*)	150	64
7	*p*-TSA	30	Ethanol: Water (3:7 *v/v*)	125	68
8	*p*-TSA	30	Ethanol: Water (4:6 *v/v*)	90	72
9	*p*-TSA	30	Ethanol: Water (5:5 *v/v*)	65	75
10	*p*-TSA	30	Ethanol: Water (6:4 *v/v*)	70	71
11	*p*-TSA	30	Ethanol: Water (7:3 *v/v*)	80	70
12	*p*-TSA	30	Ethanol: Water (8:2 *v/v*)	100	68
13	*p*-TSA	30	Ethanol: Water (9:1 *v/v*)	120	62
14	***p*-TSA**	**20**	**Ethanol: Water (5:5 *v/v*)**	**65**	**78**
15	*p*-TSA	10	Ethanol: Water (5:5 *v/v*)	65	74
16	*p*-TSA	40	Ethanol: Water (5:5 *v/v*)	70	75
17	*p*-TSA	50	Ethanol: Water (5:5 *v/v*)	70	75

*Reaction conditions: isatoic anhydride (1 mmol), 2-Furoic hydrazide (1 mmol), salicylaldehyde (1 mmol), Catalyst: *p*-TSA, Solvent: 10 mL, ultrasound sonication.

2.2. Biology

2.2.1. Mushroom tyrosinase inhibition and structure activity relationship

All newly synthesized compounds (**4a–4j**) were examine for their inhibitory potentials against tyrosinase enzyme and results were evaluated in Table 3. All these compounds showed potent inhibitory activities against tyrosinase as evident from their much lower IC_{50} (μM) values as compared to standard, kojic acid having IC_{50} value of 16.8320 ± 1.1600 μM. In present investigation, all compounds revealed much lower IC_{50} values than the standard kojic acid which signifies their potency for tyrosinase inhibition.

The structure-activity relationship (SAR) was predictable by examining the effect of different substituents on aryl group. Because, it was the only varying part in the molecule and all other parts are remains same. From the screening result, we can conclude that the 4-oxoquinazolin-3(4*H*)-yl)furan-2-carboxamides possesses electron donating moiety in their structure has higher IC_{50} value than the compound containing electron withdrawing moiety. The compounds **4f** and **4i** (except **4g**) basically bearing electron donating group shows higher IC_{50} *i.e.* 1.218 ± 0.614 and 1.775 ± 0.947 μM respectively, which is lower than that of standard kojic acid (16.8320 ± 1.1600 μM). Means they showed better tyrosinase inhibition than that of kojic acid. On the other hand compounds **4b–4e, 4h** and **4j** has electron withdrawing moiety in its structure. They have lowest IC_{50} values (0.028 ± 0.016 to 0.627 ± 0.085 μM) which are significant and superior than the standard kojic acid (16.8320 ± 1.1600 μM) and compounds **4f** and **4i**. Amongst the all synthesized and screened compounds, **4e** found to be more active against the tyrosinase inhibition. Therefore, it can be concluded that active sites of 4-oxoquinazolin-3(4*H*)-yl)furan-2-carboxamides with aryl moiety bearing electron withdrawing groups on its structure possibly interacts more with the enzyme.

2.2.2. Kinetic analysis

The kinetic study was performed to understand the inhibitory mechanism of synthetic compounds on tyrosinase inhibition. To determine the inhibition type and inhibition constant, we select most potent compound *i.e.* **4e**, Based on IC_{50} values in Table 3. The kinetic results of the enzyme involves the examination of Lineweaver-Burk plot of 1/V versus 1/[S] in the presence of different concentrations of inhibitor resulted into a series of straight lines (Fig. 2A). The results of kinetic study and plot showed that the compound **4e** intersect within the second quadrant. Whereas, V_{max} decreased with increasing doses of inhibitors and K_m remains the same. This showed that compound **4e** inhibit the tyrosinase enzyme non-competitively to form the enzyme-inhibitor complex. The enzyme inhibitor dissociation constant (*Ki*) was determining by plotting slope against the concentration of inhibitors (Fig. 2B). The Kinetic parameters for tyrosinase activity using variety of concentration of compound **4e** were represented in Table 4.

2.2.3. Free radical scavenging

DPPH assays are widely used for the assessment of the antioxidant properties of products [42,43]. All the synthesized compounds **(4a–4j)** were inspected for their DPPH free radical scavenging ability. From the results presented in the Fig. 3, we can conclude that the compounds **4f, 4g** and **4i** showed excellent activity, while other compounds did not show significant radical scavenging activity even at the high concentration (100 μg/mL).

Table 2
Library of synthesized 4-oxoquinazolin-3(4*H*)-yl)furan-2-carboxamides.

Entry	Compound structure	Code	Time (min)	Yield (%)
1.	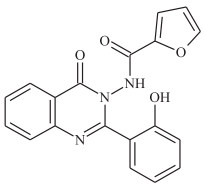	4a	65	78
2.	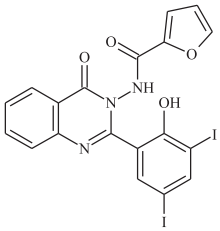	4b	55	84
3.	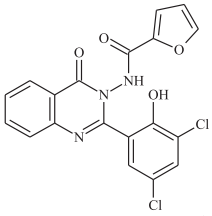	4c	55	83
4.	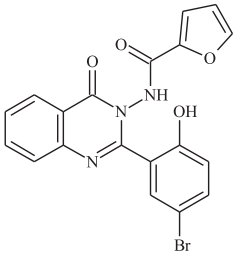	4d	65	72
5.	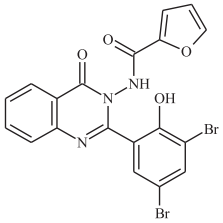	4e	60	81
6.	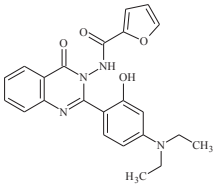	4f	70	71
7.	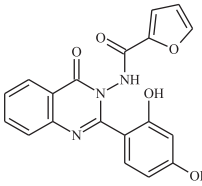	4 g	65	92
8.	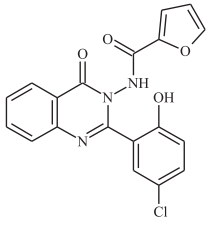	4 h	55	89

Table 2 (*continued*)

Entry	Compound structure	Code	Time (min)	Yield (%)
9.	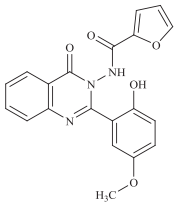	4i	70	95
10.	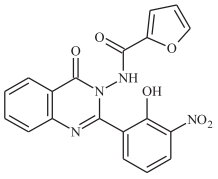	4j	70	96

*Reaction conditions: isatoic anhydride (1 mmol), 2-Furoic hydrazide (1 mmol), various salicylaldehydes (1 mmol), Catalyst: *p*-TSA (20 mol %), Solvent: Ethanol: Water (5:5 *v/v*) 10 mL, ultrasound sonication.

Table 3
IC_{50} values of compounds **(4a–4j).**

Sr. no	Compound	Tyrosinase activity IC_{50} ± SEM (μM)
1	4a	0.499 ± 0.051
2	4b	0.055 ± 0.093
3	4c	0.627 ± 0.085
4	4d	0.063 ± 0.052
5	**4e**	**0.028 ± 0.016**
6	4f	1.218 ± 0.614
7	4g	0.056 ± 0.044
8	4h	0.052 ± 0.077
9	4i	1.775 ± 0.947
10	4j	0.031 ± 0.027
11	Kojic acid	16.832 ± 1.162

SEM = Standard error of the mean; values are expressed in mean ± SEM.

2.2.4. Chemoinformatics properties and lipinski's rule of five (RO5) validation

The chemoinformatics properties of all the synthesized compounds (**4a–4j**) were predicted by using computational tools followed by validation through Lipinski rule of five (RO5) analysis. This rule states that molecular mass and log*P* values should be less than 500 g/mol and 5, respectively. Likewise, the compounds should possess no greater than 10 HBA and 5 HBD, respectively. The previous research work indicates that higher values of HBA and HBD results in poor drug permeability [44].

In the present studies, all synthesized compounds **4a–4j** obeys RO5 rule including compound **4b** and **4e** even it has little higher molecular mass of 598 and 502 g/mol, respectively. The polar surface area (PSA) is the surface sum of all polar atoms within a molecule which is frequently utilized to predict the drug ability in cell permeation. The predicted results showed that all synthesized compounds (**4a–4j**) possess less values of PSA than early reports [45,46]. Thus, predicted results on cheminformatics parameters for all compound showed that synthesized compounds **4a–4j** fall in standard range suggesting their potent oral bioactivity behavior. The estimated chemoinformatics properties of synthesized 4-oxoquinazolin-3(4*H*)-yl)furan-2-carboxamides (**4a–4j**) listed in Table 5. Drug score of target compound is collective study of the parameters such as hydrophobicity, molecule size and flexibility, hydrogen bonding characteristics along with presence of various pharmacophoric features [47]. The generated results for all synthesized compounds showed that compounds **4a–4h** exhibits good drug score values, which indicates it's drug-likeness behavior.

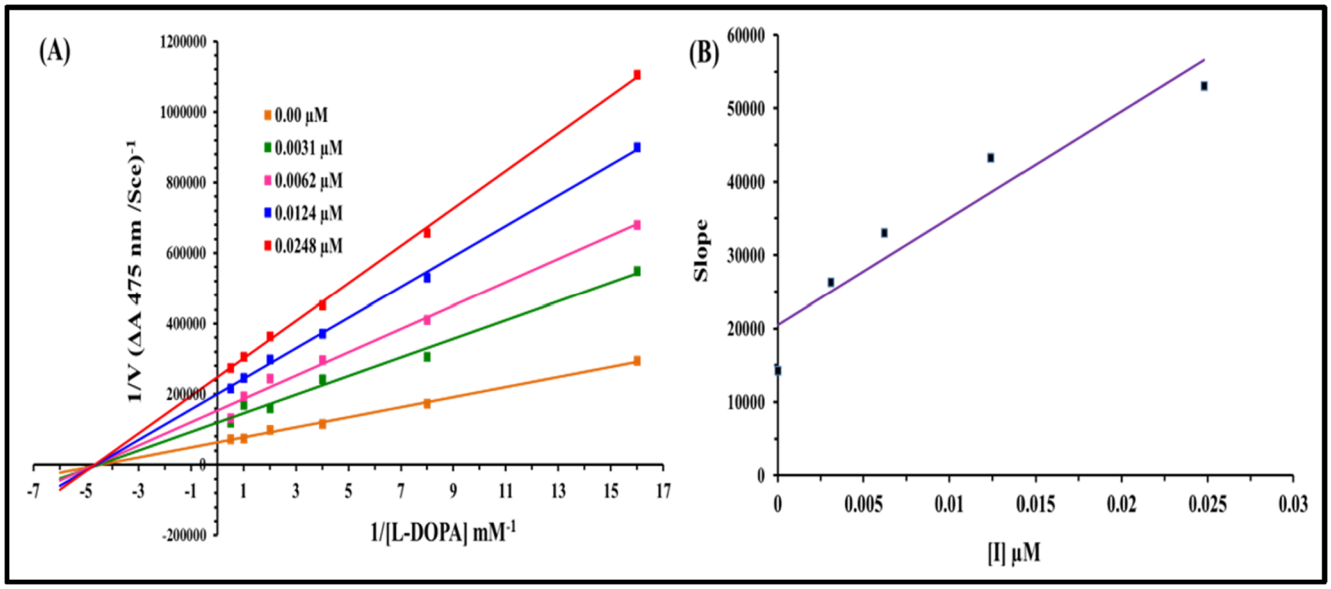

Fig. 2. (A) Lineweaver–Burk plots for inhibition of tyrosinase in the presence of Compound **4e**, concentrations of **4e** are 0.00, 0.014, 0.028 and 0.056 µM, respectively. Substrate L-DOPA Concentrations are 0.0625, 0.125, 0.25, 0.5, 1 and 2 mM, respectively. (B) The insets represents the plot of the slope versus inhibitor **4e** concentrations to determine inhibition constant. The lines were drawn using linear least squares fit.

Table 4
Kinetic parameters of the mushroom tyrosinase for L-DOPA activity in the presence of various concentrations of **4e**.

Concentration (µM)	V_{max} (ΔA /*Sec*)	K_m (mM)	Inhibition Type	*Ki* (µM)
0.00	1.07763×10^{-5}	0.67	Non-competitive	0.052
0.014	5.96971×10^{-6}	0.67		
0.028	5.12121×10^{-6}	0.67		
0.056	4.42424×10^{-6}	0.67		

V_{max} is the reaction velocity, K_m is the Michaelis-Menten constant, and *Ki* is the EI dissociation constant.

2.2.5. Molecular docking analysis

*2.2.5.1. Binding energy evaluation of synthesized compounds **4a–4j**.* To predict the best-fitted conformational position of synthesized ligands **4a–4j** within the active region of target protein, the generated docked

Table 5
Chemoinformatics properties of synthesized compounds.

Ligands	Mol. wt. (g/mol)	No. HBA	No. HBD	Mol. Log*P*	MolPSA (A^2)	Mol. Vol (A^3)	Drug Score
4a	347	5	2	2.77	76	332	1.06
4b	598	5	2	4.24	75	391	0.95
4c	415	5	2	4.08	75	364	0.86
4d	425	5	2	3.62	76	354	0.97
4e	502	5	2	4.35	75	374	0.78
4f	418	5	2	3.83	79	420	0.81
4g	363	6	3	2.51	94	343	1.41
4h	381	5	2	3.48	76	349	1.18
4i	377	6	2	2.86	84	364	0.98
4j	392	7	2	2.38	113	357	0.76

*HBA: Hydrogen Bond Acceptor, HBD: Hydrogen Bond Donor.

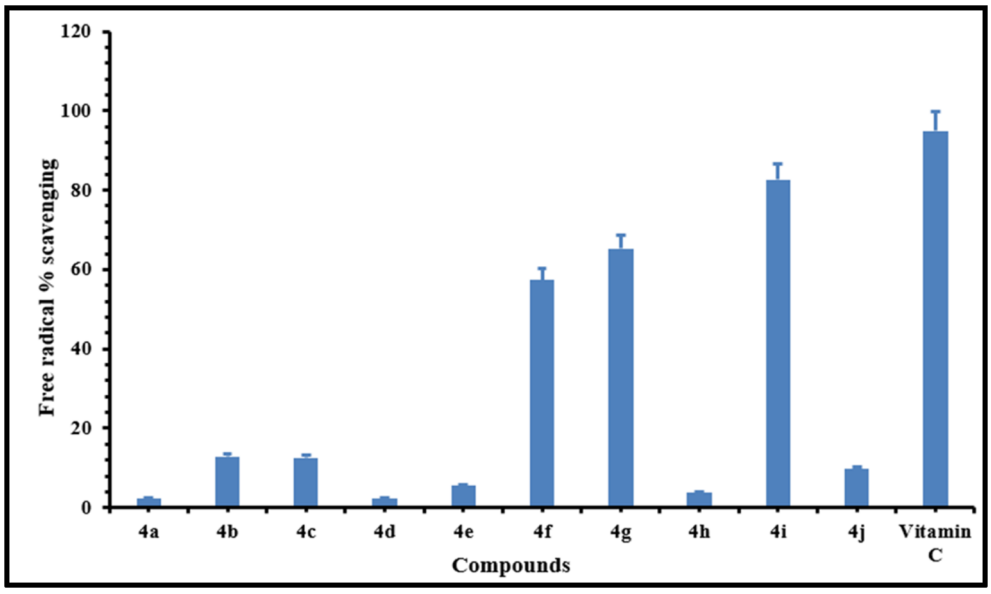

Fig 3. Free radical scavenging activity (%) of the synthesized compounds; values are presented as the mean ± SEM. All compound concentrations were 100 µg/mL.

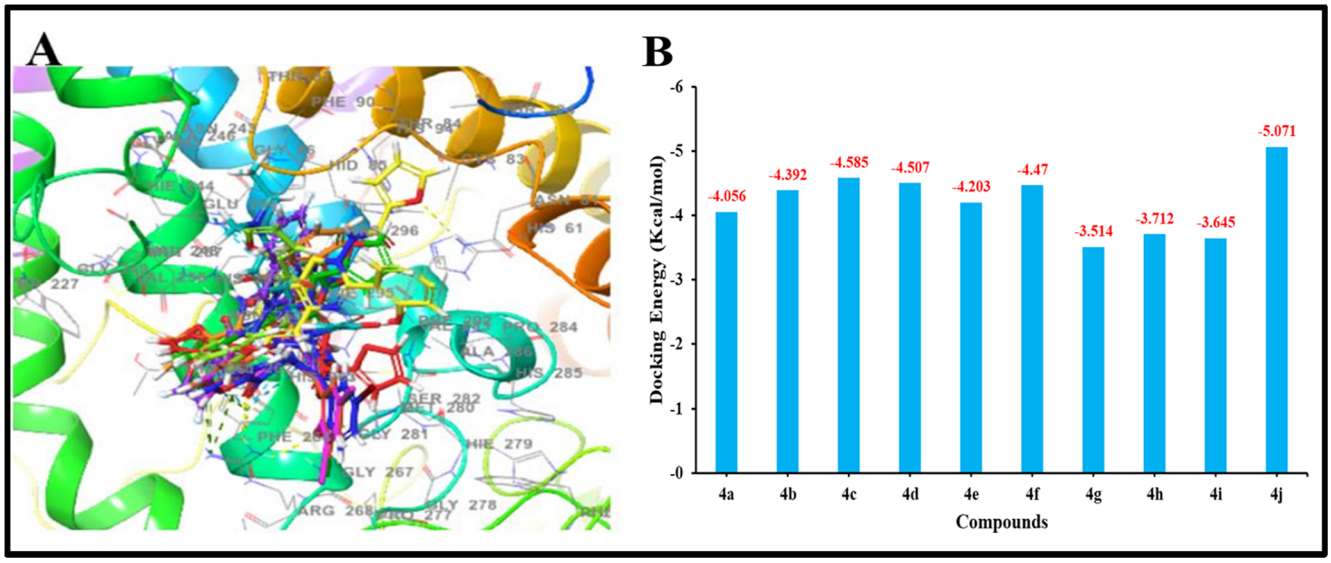

Fig 4. (A) Docking energy complexes of **4a–4j** within the active region of target protein (B) binding energy values (kcal/mol) of **4a–4j.**

complexes were analyzed on the basis of Glide docking energy values (kcal/mol) and bonding interaction (hydrogen/hydrophobic) behavior. The lowest binding energy value represents the best conformational position of ligand within the active region of target protein.

The docking results showed that all the synthesized ligands **4a–4j** were bind within the active site of target protein with different conformational poses and energy values, respectively. Fig. 4A revealed the binding pattern of all synthesized compounds **4a–4j** showed their similar conformational behavior within the active region of target protein. In addition, the binding energy values of all compounds **4a–4j** resembled to each other (Fig. 4B). The comparative results revealed that all compounds (**4a–4j**) exhibited good docking energy values. The basic skeleton of all the synthesized compounds (**4a–4j**) was similar and hence the obtained binding energy values are close to each other with no big difference.

2.2.5.2. Binding analysis of ligands against tyrosinase. Based on *in vitro* results, **4e** docking complex was assessed to understand their binding conformational analysis within active site of target protein. In detail, docking analysis one hydrogen and three π-π interactions was observed in docking complex **4e**. Fig. 5A and B signifies the 3D and 2D depictions of most active compound **4e,** respectively. The two quinazolinone rings and one furan ring interacted through π-π interactions at Hie244 and Phe264, respectively. Whereas, the hydroxyl group of benzene ring formed hydrogen bond at Asn260 with target tyrosinase protein. Literature data also ensured the importance of these residues in bonding with other tyrosinase inhibitors, which strengthen our docking results [48–50].

3. Conclusion

The successful multicomponent synthesis of 4-oxoquinazolin-3(4*H*)-yl)furan-2-carboxamides derivatives using ethanol: water (5:5 *v/v*) solvent system was carried out under ultrasound sonication. After successful synthesis, the structure of compounds was confirmed by spectral techniques such as IR, NMR and LCMS analysis. The features of this method are simple methodology, mixed green solvent, easy filtration, use of ultrasound sonication, less reaction time and higher yield of product. Along with this, all the compounds **4a − 4j** shows excellent inhibitory activity against tyrosinase enzyme. The excellent tyrosinase

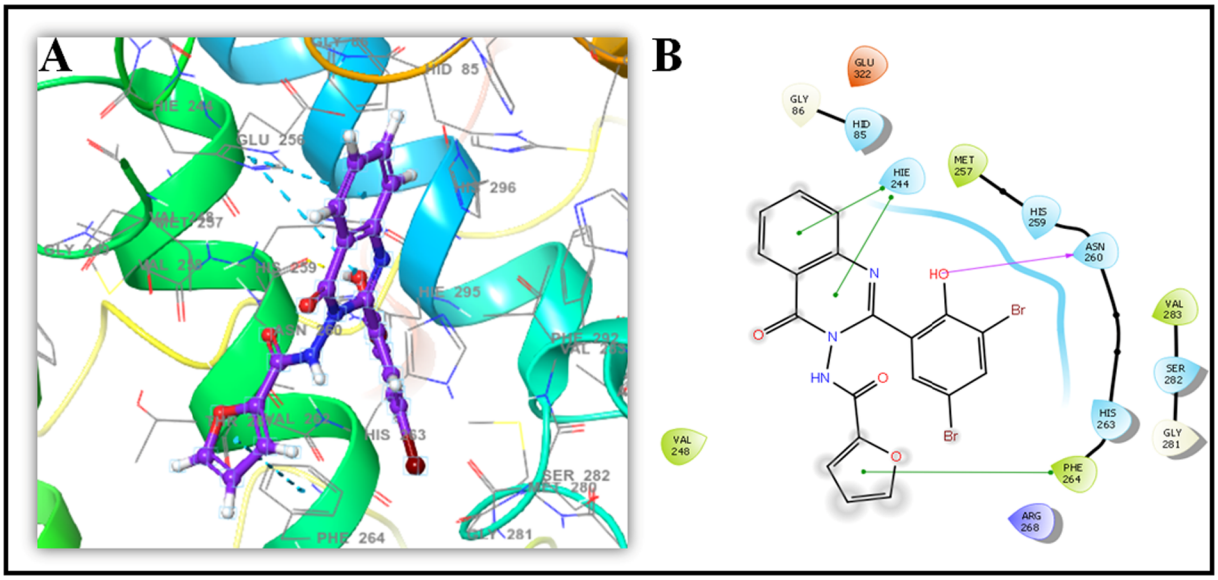

Fig 5. Docking depictions of **4e** complex against tyrosinase in 3D (A) and 2D (B).

inhibition activity response results into much lower IC_{50} values within range of 0.028 ± 0.016 to 1.775 ± 0.947 μM as compared to the standard kojic acid IC_{50} value *i.e.* 16.832 ± 1.162 μM through *in vitro* analysis. In addition, DPPH assay indicates that compounds **4f**, **4g** and **4i** shows good antioxidant properties. The *in silico* molecular docking investigation is in support of *in vitro* findings. In an overall, compound **4e** possesses extremely lower IC_{50} values against tyrosinase inhibition activity than standard kojic acid (IC_{50} value for **4e** = 0.028 ± 0.016 μM). From the results on biological activity and molecular docking study of synthesized compounds **4a–4j**, it can be concluded that these compounds can find their utility for the leading medicinal scaffolds in molecular drug designing as tyrosinase inhibitors.

4. Experimental

4.1. Chemistry

4.1.1. Materials and method

Various substituted salicylaldehydes, isatoic anhydride, 2-Furoic hydrazide and *p*-Toluene sulfonic acid (*p*-TSA) were purchased from Sigma-Aldrich, Korea and used as received without further purification. Digimelt (SRS, USA) melting point apparatus was used to measure melting point of synthesized products. The formation of products (**4a–4j**) was confirmed by spectral techniques such as IR, NMR and LCMS Analysis. IR spectra were recorded on a Frontier IR Perkin–Elmer spectrophotometer. NMR spectra were recorded on a Bruker AC-400 and Bruker Avance III 600 MHz FT-NMR spectrometer in DMSO-d_6 using tetramethylsilane as an internal standard. The LCMS spectra were recorded on a Bruker MicroTof-Q spectrometer (Germany) coupled with Dionex Ultimate 3000/LC 09115047 (USA).

4.1.2. General procedure for the synthesis of 4-oxoquinazolinone carboxamide

An equimolar amount of Isatoic anhydride (1 mmol) and 2-Furoic hydrazide (1 mmol) was taken in 50 mL round bottom flask containing 10 mL of ethanol: water (5:5 *v/v*) mixed solvent and *P*-TSA (20 mol%). The resultant reaction mixture was sonicated till the completion of reaction. Then the respective substituted salicylaldehydes (1 mmol) were added in it. The reaction mixture was further sonicated, and the progress of reaction was monitored on thin layer chromatography (TLC). After completion of reaction the product was isolated by simple filtration method and washed with ethanol. The formation of product was confirmed by spectral techniques such as IR, NMR and LCMS Analysis.

*4.1.2.1. N-[2-(2-hydroxyphenyl)-4-oxoquinazolin-3(4H)-yl]furan-2-carboxamide **(4a)***. White powder; M.P.: 168–170 °C; IR: 3401, 2851, 1621, 1607, 1478, 1368, 1310, 1273, 1227, 1201, 1149, 1083, 1013, 964, 884, 847, 775, 754 cm^{-1}; ^{1}H NMR (600 MHz, DMSO-d_6): δ 12.10 (s, 1H, –NH), 11.14 (s, 1H, –OH), 8.65 (s, 1H), 7.96 (d, 1H), 7.54 (d, 2H, J = 4 Hz), 7.30 (t, 3H, J = 8 & 4 Hz), 6.91–6.94 (m, 3H), 6.71–6.72 (m, 1H) ppm; ^{13}C NMR(150 MHz, DMSO-d_6) : δ 157.86, 154.46, 148.76, 146.76, 146.51, 131.87, 129.86, 129.85, 119.84, 119.27, 119.22, 119.21, 116.88, 115.69, 112.62 ppm; LCMS (ESI): 348.1795 (M + H) and 289 (M + K), *m/z*.

*4.1.2.2. N-[2-(2-hydroxy-3,5-diiodophenyl)-4-oxoquinazolin-3(4H)-yl]furan-2-carboxamide **(4b)***. Beige powder; M.P.: above 260 °C; IR: 3409, 3199, 2987, 2854, 1651, 1620, 1591, 1541, 1477, 1434, 1367, 1298, 1270, 1186, 1156, 1083, 1033, 1014, 961, 884, 848, 769, 757, 738 cm^{-1}; ^{1}H NMR(600 MHz, DMSO-d_6): δ 12.77 (s, 1H, –NH), 12.54 (s, 1H, –OH), 8.44 (s, 1H), 8.04 (d, 1H, J = 1.2 Hz), 7.99 (d, 1H, J = 0.8 Hz), 7.84 (d, 2H, J = 1.2 Hz), 7.37 (d, 2H, J = 4 Hz), 6.73–6.74 (m, 2H) ppm; ^{13}C NMR(150 MHz, DMSO-d_6) : δ 157.01, 154.54, 147.71, 147.01, 146.90, 146.29, 139.20, 139.20, 120.87, 116.47, 112.80, 88.19, 82.52 ppm; LCMS (ESI): 597. 85(M − H) and 599 (M^+), *m/z*.

*4.1.2.3. N-[2-(3,5-dichloro-2-hydroxyphenyl)-4-oxoquinazolin-3(4H)-yl]furan-2-carboxamide **(4c)***. Beige powder; M.P.: 234–236 °C; IR: 3572, 3388, 3275, 3072, 1673, 1661, 1605, 1589, 1530, 1475, 1454, 1388, 1360, 1347, 1306, 1284, 1223, 1182, 1154, 1105, 1027, 1013, 977, 936, 847, 763, 748, 736, 707 cm^{-1}; ^{1}H NMR(400 MHz, DMSO-d_6): δ 12.57 (s, 1H, –NH), 12.37 (s, 1H, –OH), 8.59 (s, 1H), 8.02 (m, 1H), 7.66 (d, 3H, J = 4 Hz), 7.38 (s, 2H), 7.75 – 6.76 (m, 2H) ppm; ^{13}C NMR (100 MHz, DMSO-d_6) : δ 154.58, 152.64, 147.49, 147.45, 147.44, 147.41, 146.91, 146.33, 130.77, 130.73, 128.80, 128.74, 123.48, 122.03, 121.39, 116.44, 116.42, 116.41, 112.78 ppm; LCMS (ESI): 416 (M^+) and 417(M − H) for 1 × 35.5Cl, 1 × 37Cl *m/z*.

*4.1.2.4. N-[2-(5-bromo-2-hydroxyphenyl)-4-oxoquinazolin-3(4H)-yl]furan-2-carboxamide **(4d)***. White powder; M.P.: 209–212 °C; IR: 3386, 3134, 3003, 2873, 1652, 1620, 1480, 1463, 1356, 1321, 1268, 1199, 1086, 957, 849, 766, 745, 697 cm^{-1}; ^{1}H NMR (600 MHz, DMSO-d_6): δ 12.20 (s, 1H, –NH), 11.16 (s, 1H, –OH), 8.62 (s, 1H), 7.98 (m, 1H), 7.78 (d, 1H, J = 4 Hz), 7.42–7.45 (m, 2H), 7.35 (d, 1H, J = 4 Hz), 6.91 (d, 2H, J = 8 Hz), 6.72–6.74 (m, 2H) ppm; ^{13}C NMR(150 MHz, DMSO-d_6) : δ 156.82, 154.58, 146.69, 146.68, 146.58, 146.09, 134.04, 130.76, 121.87, 119.14, 115.81, 112.61, 110.95 ppm; LCMS (ESI): 425 (M − H), 449 (M + Na) for isotope 81Br, 425.9890 (M − H) for isotope 81Br and 386.8627 (M − K) for isotope 79Br *m/z*.

*4.1.2.5. N-[2-(3,5-dibromo-2-hydroxyphenyl)-4-oxoquinazolin-3(4H)-yl]furan-2-carboxamide **(4e)***. White powder; M.P.: 263–265 °C; IR: 3214, 3069, 1751, 1657, 1603, 1588, 1530, 1470, 1445, 1428, 1348, 1291, 1272, 1223, 1170, 1106, 1008, 963, 871, 852, 760, 737, 687 cm^{-1}; ^{1}H NMR (400 MHz, DMSO-d_6): δ 12.60 (s, 2H, –NH & –OH), 8.55 (s, 1H), 8.02 (m, 1H), 7.79 – 7.84 (m, 3H), 7.38–7.39 (m, 2H), 6.75–6.76 (m, 2H) ppm; ^{13}C NMR(100 MHz, DMSO-d_6) : δ 154.53, 154.02, 147.54, 146.96, 146.26, 136.03, 132.49, 121.51, 116.51, 112.81, 111.72, 110.92 ppm; LCMS (ESI): 480.8373 (M − Na) and 504.8530(M + H) *m/z*.

*4.1.2.6. N-(2-(4-(diethylamino)-2-hydroxyphenyl)-4-oxoquinazolin-3(4H)-yl)furan-2-carbox -amide **(4f)***. Yellow powder; M.P.: 192–194 °C; IR: 3208, 3049, 2969, 2930, 1625, 1599, 1518, 1477, 1412, 1351, 1340, 1292, 1242, 1223, 1179, 1130, 1084, 1005, 968, 702 cm^{-1}; ^{1}H NMR (400 MHz, DMSO-d_6): δ 11.83 (s, 1H, –NH), 11.33 (s, 1H, –OH), 8.43 (s, 1H), 7.94–7.95 (m, 1H), 7.18–7.26 (m, 3H), 6.70–6.71 (m, 2H), 6.26–6.29 (m, 1H), 6.13 (d, 2H, J = 4 Hz), 3.36–3.40 (q, 4H), 1.11 (t, 6H, J = 8 Hz) ppm; ^{13}C NMR(100 MHz, DMSO-d_6) : δ 160.09, 153.93, 150.65, 150.47, 147.06, 146.13, 132.00, 115.02, 112.53, 106.92, 104.15, 97.94, 44.27, 13.01 ppm; LCMS (ESI): 496 (M - Na) *m/z*.

*4.1.2.7. N-[2-(2,4-dihydroxyphenyl)-4-oxoquinazolin-3(4H)-yl]furan-2-carboxamide **(4g)***. Yellow powder; M.P.: 200–203 °C; IR: 3209, 3050, 2969, 2930, 1626, 1589, 1517, 1476, 1412, 1351, 1291, 1243, 1222, 1179, 1128, 1083, 1005, 967, 883, 852, 784, 754, 703, 680 cm^{-1}; ^{1}H NMR(600 MHz, DMSO-d_6): δ 11.91 (s, 1H, –NH), 11.71 (s, 1H, –OH), 11.34 (s, 1H, –OH), 7.91–7.93 (m, 2H), 7.72–7.75 (m, 1H), 7.24–7.30 (m, 2H), 7.16 (d, 1H, J = 12 Hz), 6.69–6.70 (m, 1H), 6.35–6.37 (m, 1H), 6.32 (d, 1H) ppm; ^{13}C NMR(150 MHz, DMSO-d_6) : δ 165.64, 163.71, 161.23, 160.32, 159.90, 154.21, 149.74, 147.55, 146.93, 146.26, 141.87, 137.39, 131.73, 129.40, 123.98, 115.81, 115.32, 112.55, 111.04, 110.71, 109.10, 108.21, 103.14, 102.67 ppm; MS (EI): 365 (M + 2), *m/z*.

*4.1.2.8. N-[2-(5-chloro-2-hydroxyphenyl)-4-oxoquinazolin-3(4H) yl]furan-2-carboxamide **(4h)***. White powder; M.P.: 193–195 °C; IR: 3386, 3210, 3136, 2971, 2871, 1647, 1622, 1592, 1482, 1463, 1355, 1324, 1267, 1243, 1198, 1085, 1016, 958, 918, 884, 851, 827, 761, 747, 716 cm^{-1}; ^{1}H NMR(400 MHz, DMSO-d_6): δ 12.20 (s, 1H, –NH), 11.15 (s, 1H, –OH),

8.63 (s, 1H), 7.98–7.99 (m, 1H), 7.66 (d, 2H, J = 4 Hz), 7.31–7.35 (m, 3H), 6.95–6.97 (d, 1H, J = 8 Hz), 6.72–6.75 (q, 2H) ppm; ^{13}C NMR (100 MHz, DMSO-d_6) : δ 165.55, 160.33, 156.41, 154.57, 146.69, 146.60, 146.21, 146.21, 141.88, 137.41, 131.24, 129.41, 127.88, 123.99, 123.49, 121.27, 118.69, 115.81, 112.62 110.73 ppm; LCMS (ESI): 382 (M^+), *m/z*.

*4.1.2.9. N-[2-(2-hydroxy-5-methoxyphenyl)-4-oxoquinazolin-3(4H)-yl] furan-2-carboxamide (**4i**)*. White powder; M.P.: 180–182 °C; IR: 3118, 2968, 1767, 1732, 1497, 1457, 1360, 1322, 1274, 1197, 1163, 1127, 1044, 1015, 959, 851, 812, 766, 745, 682 cm^{-1}; ^{1}H NMR(600 MHz, DMSO-d_6): δ 12.07 (s, 1H, –NH), 11.71 (s, 1H, –OH), 8.63 (s, 1H), 7.91–7.95 (m, 1H), 7.74 (s, 1H), 7.32 (s, 1H), 7.25 (t, 1H, J = 6 Hz), 7.15–7.17 (d, 1H, J = 12 Hz), 7.11 (d, 1H), 6.90–6.92 (m, 1H), 6.86(d, 1H, J = 12 Hz), 6.71–6.72 (q, 1H), 3.73 (s, 3H), ppm; ^{13}C NMR (150 MHz, DMSO-d_6) : δ 160.34, 152.61, 151.86, 147.56, 146.50, 141.87, 137.40, 129.40, 123.98, 118.74, 117.74, 115.79, 112.61, 110.74, 55.98 ppm; LCMS (ESI): 376 (M − H), *m/z*.

*4.1.2.10. N-(2-(2-hydroxy-3-nitrophenyl)-4-oxoquinazolin-3(4H)-yl)furan-2-carboxamide (**4j**)*. Light Yellow powder; M.P.: 188–190 °C; IR: 3556, 3128, 2969, 1765, 1729, 1670, 1621, 1592, 1528, 1467, 1360, 1299, 1272, 1250, 1197, 1082, 1011, 979, 848, 760, 741, 681 cm^{-1}; ^{1}H NMR (600 MHz, DMSO-d_6): δ 12.72 (s, 1H, –NH), 11.44 (s, 1H, –OH), 8.72 (s, 1H), 8.01 (t, 1H, J = 6 Hz), 7.92 (d, 2H, J = 6 Hz), 7.72–7.75 (q, 1H), 7.37 (s, 1H), 7.25 (t, 1H, J = 6 Hz), 7.11–7.17 (m, 2H), 6.73–6.74 (q, 1H) ppm; ^{13}C NMR(150 MHz, DMSO-d_6) : δ 160.31, 154.56, 151.98, 147.54, 147.36, 147.35, 146.84, 146.39, 141.87, 138.08, 137.39, 135.38, 129.40, 127.00, 123.98, 122.27, 119.71, 116.34, 115.81, 112.76, 110.71 ppm; LCMS (ESI): 391 (M − H), *m/z*.

4.2. Biology

4.2.1. In vitro methodology

4.2.1.1. Mushroom tyrosinase activity. The mushroom tyrosinase (Sigma Chemical, USA) inhibition study was executed according to previously reported methods [51–53] of our group. In detail, phosphate buffer (140 µL, 20 mM, pH 6.8), mushroom tyrosinase (20 µL, 30 U/mL) and inhibitor solution (20 µL) were taken in the wells of a 96-well microplate and pre-incubated for 10 min at room temperature. At that time, 3,4-dihydroxyphenylalanine *i.e.* L-DOPA (Sigma Chemical, USA, 20 µL, 0.85 mM) was added to it and the assay plate was further incubated at 25 °C for 20 min. Subsequently, the microplate reader (OPTI Max, Tunable) was used to measure the absorbance at 475 nm. In this experiment, phosphate buffer was used as a negative control while Kojic acid was used as a reference inhibitor. The amount of inhibition by the test compounds was expressed in terms of the percentage of concentration necessary to achieve 50% inhibition *i.e.* IC_{50}. The experimental study was done in three independent experiments. IC_{50} values were calculated by nonlinear regression using GraphPad Prism 5.0.

The % inhibition of tyrosinase was calculated using following Eq. (1),

$$\text{Inhibition}\ (\%) = [(B - S)/B] \times 100 \quad (1)$$

where the B and S are the absorbance for the blank and samples, respectively.

4.2.1.2. Kinetic analysis of inhibition of tyrosinase. The most potent compound **4e** was selected on the basis of IC_{50} value for kinetic analysis. The already reported methods were accessed to execute the series of experiments to determine the inhibition kinetics of **4e** [48,49]. The inhibitor concentrations for **4e** were 0.00, 0.014, 0.028 and 0.056 µM. The concentrations of substrate L-DOPA used in this kinetic study was in the range of 0.0625–2 mM. The Pre-incubation and measurement time were the same as discussed in the mushroom tyrosinase inhibition assay protocol. After the addition of enzyme, the initial linear portion of absorbance used to determine the maximal initial velocity up to five minutes at a 30 s interval. The Lineweaver–Burk plots of inverse of velocities ($1/V$) versus inverse of substrate concentration $1/[\text{L-DOPA}]$ mM^{-1} was used to determine the inhibition type of the enzyme. The secondary plot of $1/V$ against inhibitors concentrations assessed to evaluate EI dissociation constant (Ki).

4.2.1.3. Free radical scavenging assay. The already reported method was modified to screen the Radical scavenging activity [42,43] using 2, 2-diphenyl-1 picrylhydrazyl (DPPH) assay. The assay solution consisted of 100 µL DPPH (150 µM) and 20 µL increasing concentration of test compounds. The total volume in each well was adjusted to 200 µL with methyl alcohol followed by incubation for 30 min at room temperature. Ascorbic acid (Vitamin C) was used as a reference inhibitor. The microplate reader (OPTI Max, Tunable) assay used for measurements at 517 nm. The rate of reaction was compared, and the percent inhibition caused by the presence of tested inhibitors was calculated in this assay. Each concentration was analyzed in three independent experiments.

4.2.2. In silico analysis: computational methodology

4.2.2.1. Selection of mushroom tyrosinase structure from PDB. The Protein Data Bank (PDB) (http://www.rcsb.org) was referred to retrieve three dimensional (3D) structure of mushroom tyrosinase (*Agaricus bisporus*) (PDBID: 2Y9X). The selected protein was energy minimized by employing conjugate gradient algorithm and amber force field in UCSF Chimera 1.10.1 [54,55].

4.2.2.2. Grid generation and molecular docking. Before the molecular docking experiment few things were adjusted in the protein structure to get better docking results. The “Protein Preparation Wizard” by Maestro interface in Schrödinger Suite was used to prepare the tyrosinase structure. Initially, bond orders were assigned and hydrogen atoms were added to the protein structure. After that, the structure was minimized to reach the converged root mean square deviation (RMSD) of 0.30 Å with the OPLS_2005 force field. The active site of the enzyme (tyrosinase) was defined by co-crystallized ligands from Protein Data Bank and literature survey [48–50]. The synthesized ligands **4a–4j** were sketched in 2D sketcher in Schrödinger Suite and saved in Maestro interface for docking experiment. The molecular docking experiment was performed for all the synthesized ligands against target protein using Glide docking protocol [54] to predict the binding energies (docking scores) and conformational positions of ligands within active region of protein. Throughout the docking simulations, both partial flexibility and full flexibility around the active site residues are performed by Glide/SP/XP and induced fit docking (IFD) approaches [55].

Declaration of Competing Interest

The authors declare no conflict of interests

References

[1] M.A. Birch-Machin, A. Bowman, Oxidative stress and ageing, Br. J. Dermatol. 175 (2016) 26–29.
[2] J.Y. Bae, S.S. Lim, S.J. Kim, J.S. Choi, J. Park, S.M. Ju, S.J. Han, I.J. Kang, Y.H. Kang, Bog blueberry anthocyanins alleviate photoaging in ultraviolet-B irradiation-induced human dermal fibroblasts, Mol. Nutr. Food Res. 53 (2009) 726–738.
[3] F. Giampieri, J.M. Alvarez-Suarez, S. Tulipani, A.M. Gonzales-Paramas, C. Santos-Buelga, S. Bompadre, J.L. Quiles, B. Mezzetti, M.J. Battino, Photoprotective potential of strawberry (Fragaria × ananassa) extract against UV-A irradiation damage on human fibroblasts, Agric. Food Chem. 60 (2012) 2322–2327.
[4] K. Tarangini, S. Mishra, Production, characterization and analysis of melanin from isolated marine pseudomonas sp. using vegetable waste, Res. J. Engineering. Sci., 2 (2013) 40–46.
[5] H.Y. Park, M. Kosmadaki, M. Yaar, B.A. Gilchrest, Cellular mechanisms regulating

human melanogenesis, Cell. Mol. Life Sci. 66 (2009) 1493–1506.
[6] Q.X. Chen, I. Kubo, Kinetics of mushroom tyrosinase inhibition by quercetin, J. Agric. Food Chem. 50 (2002) 4108–4112.
[7] S. Briganti, E. Camera, M. Picardo, hemical and instrumental approaches to treat hyperpigmentation, Pigment Cell Res. 16 (2003) 101–110.
[8] A. Slominski, D.J. Tobin, S. Shibahara, J. Wortsman, Melanin pigmentation in mammalian skin and its hormonal regulation, Physiol Rev. 84 (2004) 1155–1228.
[9] V.E. Nikitina, E.P. Vetchinkina, E.G. Ponomareva, Y.V. Gogoleva, Phenol oxidase activity in bacteria of the genus Azospirillum, Microbiol. 79 (2010) 327–333.
[10] S. Piñero, J. Rivera, D. Romero, M.A. Cevallos, A. Martínez, F. Bolívar, G.J. Gosset, Tyrosinase from rhizobium etli is involved in nodulation efficiency and symbiosis-associated stress resistance, Mol. Microbiol. Biotechnol. 13 (2007) 35–44.
[11] J. Michalik, W. Emilianowicz-Czerska, L. Switalski, K. Raczyńska-Bojanowska, Monophenol monooxygenase and lincomysin biosynthesis in streptomyces lincolnensis, Agents Chemother. 8 (1975) 526–531.
[12] D.B. Mosher, M.A. Pathak, T.B. Fitzpatrick, Vitiligo, etiology, pathogenesis, diagnosis, and treatment, in: T.B. Fitzpatrick, A.Z. Eisen, K. Wolff, I.M. Freedberg, K.F. Austen (Eds.), Update: Dermatology in General Medicine, McGraw-Hill, New York, 1983, pp. 205–225.
[13] K. Maeda, M. Fukuda, In Vitro effectiveness of several whitening cosmetic components in human melanocytes, J. Soc. Cosmet. Chem. 42 (1991) 361–368.
[14] E. Jafari, M.R. Khajouei, F. Hassanzadeh, G.H. Hakimelahi, G.A. Khodarahmi, Quinazolinone and quinazoline derivatives: recent structures with potent antimicrobial and cytotoxic activities, Res. Pharm. Sci. 11 (2016) 1–14.
[15] (a) A. Hameed, M. Al-Rashida, M. Uroos, S. Abid Ali, M. Arshia, K.M. Khan Ishtiaq, Quinazoline and quinazolinone as important medicinal scaffolds: a comparative patent review (2011–2016), Expert. Opin. Ther. Pat. 28 (2018) 281–297;
(b) D. He, M. Wang, S. Zhao, Y. Shu, H. Zeng, C. Xiao, C. Lu, Y. Liu, Pharmaceutical prospects of naturally occurring quinazolinone and its derivatives, Fitoterapia 119 (2017) 136–149.
[16] (a) B. Dash, S. Dash, D. Laloo, C. Medhi, Design, synthesis and preliminary pharmacological screening (antimicrobial, analgesic and anti-inflammatory activity) of some novel quinazoline derivatives, J. Appl. Pharm. Sci. 7 (2017) 83–96;
(b) M. Dinari, F. Gharahi, P. Asadi, Synthesis, spectroscopic characterization, antimicrobial evaluation and molecular docking study of novel triazine–quinazolinone based hybrids, J. Mol. Struct. 1156 (2018) 43–50.
[17] (a) N. Jain, J. Jaiswal, A. Pathak, P.K. Singour, Synthesis, molecular docking and evaluation of 3 -{4 - [2 - amino - 4 - (substituted phenyl) - 2H - [1, 3]oxazin /thiazin-6-yl}- 2 - phenyl - 3H -quinazolin-4-one derivatives for their anticonvulsant activity, Cent. Nerv. Syst. Agents. Med Chem. 18 (2018) 63–73;
(b) S.K. Kashawa, V. Kashawa, P. Mishra, N.K.a. Jain, J.P. Stables, Synthesis anticonvulsant and CNS depressant activity of some new bioactive 1-(4-substitutedphenyl)-3-(4-oxo-2-phenyl/ethyl-4H-quinazolin-3-yl)-urea, Eur. J. Med. Chem. 44 (2009) 4335–4343.
[18] A.M. Alaa, L.A. Abou-Zeid, K.E.H. ElTahir, R.R. Ayyad, A.-A. Magda, A.S. El-Azab, Synthesis, anti-inflammatory, analgesic, COX-1/2 inhibitory activities and molecular docking studies of substituted 2-mercapto-4 (3H)-quinazolinones, Eur. J. Med. Chem. 121 (2016) 410–421.
[19] (a) L. Yang, S. Ge, J. Huang, X. Bao, Synthesis of novel (E)-2-(4-(1H–1, 2, 4-triazol-1-yl) styryl)-4-(alkyl/arylmethyleneoxy) quinazoline derivatives as antimicrobial agents, Mol. Divers. 22 (2018) 71–82;
(b) H.A. Abuelizz, R.A. El-Dib, M. Marzouk, R. Al-Salahi, In vitro evaluation of new 2-phenoxy-benzo [g][1,2,4] triazolo [1,5-a] quinazoline derivatives as antimicrobial agents, Microb. Pathog. 117 (2018) 60–67;
(c) H. Ighachane, M.H. Sedra, H. Lazrek, Synthesis and evaluation of antifungal activities of (3H)-quinazolin-4-one derivatives against tree plant fungi, J. Mater. Environ. Sci. 8 (2017) 134–143.
[20] (a) M. Hrast, K. Rožman, M. Jukič, D. Patin, S. Gobec, M. Sova, Synthesis and structure–activity relationship study of novel quinazolinone based inhibitors of Mur A, Bioorg. Med. Chem. Lett. 27 (2017) 3529–3533;
(b) F. Ding, Y. Zhan, X. Lu, Y. Sun, Recent advances in near-infrared II fluorophores for multifunctional biomedical imaging, Chem. Sci. 9 (2018) 4370–4380.
[21] (a) S.Y. Abbas, K.A. El-Bayouki, W.M. Basyouni, E.A. Mostafa, New series of 4(3H)-quinazolinone derivatives: syntheses and evaluation of antitumor and antiviral activities, Med. Chem. Res. 27 (2018) 571–582;
(b) W. Dohle, F.L. Jourdan, G. Menchon, A.E. Prota, P.A. Foster, P. Mannion, E. Hamel, M.P. Thomas, P.G. Kasprzyk, E. Ferrandis, Quinazolinone based anticancer agents: synthesis, antiproliferative SAR, antitubulin activity, and tubulin cocrystal structure, J. Med. Chem. 61 (2018) 1031–1044;
(c) F. Ding, Y. Fan, Y. Sun, F. Zhang, Beyond 1000 nm emission wavelength: recent advances in organic and inorganic emitters for deep-tissue molecular imaging, Adv. Healthcare. Mater 8 (2019) 1900260.
[22] (a) A.L. Leivers, M. Tallant, J.B. Shotwell, S. Dickerson, M.R. Leivers, O.B. McDonald, J. Gobel, K.L. Creech, S.L. Strum, A. Mathis, S. Rogers, C.B. Moore, J. Botyanszki, Discovery of selective small molecule type III Phosphatidylinositol 4-kinase alpha (PI4KIIIα) inhibitors as anti-hepatitis C (HCV) agents, J. Med. Chem. 57 (2014) 2091–2106;
(b) Z.W. Wang, M.X. Wang, X. Yao, Y. Li, J. Tan, L.Z. Wang, W.T. Qiao, Y.Q. Geng, Y.X. Liu, Q.M. Wang, Design, synthesis and antiviral activity of novel quinazolinones, Eur. J. Med. Chem. 53 (2012) 275–282.
[23] (a) C. Carmi, E. Galvani, F. Vacondio, S. Rivara, A. Lodola, S. Russo, S. Aiello, F. Bordi, G. Costantino, A. Cavazzoni, R.R. Alfieri, A. Ardizzoni, P.G. Petronini, M. Mor, Irreversible inhibition of epidermal growth factor receptor activity by 3-aminopropanamides, J. Med. Chem. 55 (2012) 2251–2264;
(b) F. Ding, S. Chen, W. Zhang, Y. Tu, Y. Sun, UPAR targeted molecular imaging of cancers with small molecule-based probes, Bioorg. Med. Chem 25 (2017) 5179–5184.
[24] X. Zhan, Y. Xu, Q. Qi, Y. Wang, H. Shi, Z. Mao, Synthesis, cytotoxic, and antibacterial evaluation of quinazolinone derivatives with substituted amino moiety, Chem. Biodivers. 15 (2018) e1700513.
[25] (a) I. Khan, A. Ibrar, N. Abbas, A. Saeed, Recent advances in the structural library of functionalized quinazoline and quinazolinone scaffolds: synthetic approaches and multifarious applications, Eur. J. Med. Chem. 76 (2014) 193–244;
(b) I. Khan, A. Ibrar, W. Ahmed, A. Saeed, Synthetic approaches, functionalization and therapeutic potential of quinazoline and quinazolinone skeletons: the advances continue, Eur. J. Med. Chem. 90 (2015) 124–169;
(c) I. Khan, S. Zaib, S. Batool, N. Abbas, Z. Ashraf, J. Iqbal, A. Saeed, Quinazolines and quinazolinones as ubiquitous structural fragments in medicinal chemistry: an update on the development of synthetic methods and pharmacological diversification, Bioorg. Med. Chem. 24 (2016) 2361–2381.
[26] (a) E. Mentese, N. Karaali, G. Akyuz, F. Yilmaz, S. Ulker, B. Kahveci, Synthesis and evaluation of α-glucosidase and pancreatic lipase inhibition by quinazolinone-coumarin hybrids, Chem. Heterocycl. Compd. 52 (2016) 1017–1024;
(b) F. Ding, C. Li, Y. Xu, J. Li, H. Li, G. Yang, Y. Sun, PEGylation regulates self-assembled small-molecule dye-based probes from single molecule to nanoparticle size for multifunctional NIR-II bioimaging, Adv. Healthcare. Mater 7 (2018) 1800973.
[27] (a) D. Wang, F. Gao, Quinazoline derivatives: synthesis and bioactivities, Chem. Cent. J. 7 (2013) 95;
(b) Y. Sun, F. Ding, Z. Zhou, C. Li, M. Pu, Y. Xu, Y. Zhan, X. Lu, H. Li, G. Yang, Y. Sun, P.J. Stang, Rhomboidal Pt(II) metallacycle-based NIR-II theranostic nanoprobe for tumor diagnosis and image-guided therapy, Proc. Natl. Acad. Sci. USA 116 (2019) 1968–1973.
[28] M.M. Ghorab, Z.H. Ismail, A.A. Radwan, M. Abdalla, Synthesis and pharmacophore modeling of novel quinazolines bearing a biologically active sulfonamide moiety, Acta Pharm. 63 (2013) 1–18.
[29] I. Khan, A. Ibrar, N. Abbas, A. Saeed, Recent advances in the structural library of functionalized quinazoline and quinazolinone scaffolds: synthetic approaches and multifarious applications, Eur. J. Med. Chem. 76 (2014) 193–244.
[30] I. Khan, A. Ibrar, W. Ahmed, A. Saeed, Synthetic approaches, functionalization and therapeutic potential of quinazoline and quinazolinone skeletons: the advances continue, Eur. J. Med. Chem. 90 (2015) 124–169.
[31] I. Khan, S. Zaib, S. Batool, N. Abbas, Z. Ashraf, J. Iqbal, A. Sameed, Quinazolines and quinazolinones as ubiquitous structural fragments in medicinal chemistry: an update on the development of synthetic methods and pharmacological diversification, Bioorg. Med. Chem. 24 (2016) 2361–2381.
[32] a) S.Y. Abbas, K.A.M. El-Bayouki, W.M. Basyouni, Utilization of isatoic anhydride in the syntheses of various types of quinazoline and quinazolinone derivatives, Synth. Commun. 46 (2016) 993–1035;
b) H.S. Bhatti, S. Seshadri, Synthesis and fastness properties of styryland azo disperse dyes derived from 6-nitrosubstituted 3-aryl-2-methyl-4(3H)-quinazolinone, Color. Technol. 120 (2004) 151–155.
[33] Q. Li, Y. Huang, T. Chen, Y. Zhou, Q. Xu, S.-F. Yin, L.-B. Han, Copper-Catalyzed Aerobic Oxidative Amination of sp3C − H Bonds: Efficient Synthesis of 2-Hetarylquinazolin-4(3H)-ones, Org. Lett. 16 (2014) 3672–3675.
[34] K.S. Suslick, L.A. Crum, Sonochemistry and Sonoluminescence Vol. 1 Wiley-Interscience, New York, 1997.
[35] G. Chatel, L. Leclerc, E. Naffrechoux, C. Bas, N. Kardos, C. Goux-Henry, B. Andrioletti, M. Draye, Ultrasonic properties of hydrophobic bis(trifluoromethylsulfonyl)imide-based ionic liquids, J. Chem Eng. Data. 57 (2012) 3385–3390.
[36] M. Draye, J.P. Bazureau. Ultrasound and microwaves: recent advances in organic chemistry. Research Signpost (2012) doi: hal-00708455.
[37] A. Maleki, J. Rahimi, O.M. Demchuk, A.Z. Wilczewska, R. Jasiński, Green in water sonochemical synthesis of tetrazolopyrimidine derivatives by a novel core-shell magnetic nanostructure catalyst, Ultrason. Sonochem. 43 (2018) 262–271.
[38] N.C. Dige, D.M. Pore, Green aspect for multicomponent synthesis of spiro[4H-indeno[1,2-b]pyridine-4,3′-[3H]indoles], Synth. Commun. 45 (2015) 2498–2510.
[39] N.C. Dige, P.G. Mahajan, D.M. Pore, Serendipitous formation of novel class of dichromenopyrano pyrimidinone derivatives possessing anti-tubercular activity against M. tuberculosis $H_{37}Rv$, Med. Chem. Res. 27 (2018) 224–233.
[40] (a) N.C. Dige, S.N. Korade, D.M. Pore, Design of task-specific ionic liquid, 1-(ethylaceto acetate)-1-(2-hydroxyethyl) piperidinium tetrachloroaluminate for multicomponent synthesis of 3,3′-disubstituted oxindoles, Res. Chem. Intermed. 43 (2017) 7029–7040;
(b) P.G. Mahajan, N.C. Dige, B.D. Vanjare, H. Raza, M. Hassan, S.-Y. Seo, C.-H. Kim, K.H. Lee, Facile synthesis of new quinazolinone benzamides as potent tyrosinase inhibitors: Comparative spectroscopic and molecular docking studies, J. Mol. Struct. (2019), https://doi.org/10.1016/j.molstruc.2019.126915.
[41] N.C. Dige, J.D. Patil, D.M. Pore, Dicationic 1,3-bis(1-methyl-1H-imidazol-3-ium) propane copper(I) dibromate: novel heterogeneous catalyst for 1,3-dipolar cycloaddition, Catal. Lett. 147 (2017) 301–309.
[42] C.V.K. Reddy, D. Sreeramulu, M. Raghunath, Antioxidant activity of fresh and dry fruits commonly consumed in India, Food Res. Int. 43 (2010) 285–288.
[43] A. Saeed, P.A. Mahesar, P.A. Channar, F.A. Larik, Q. Abbas, M. Hassan, H. Raza, S.Y. Seo, Hybrid pharmacophoric approach in the design and synthesis of coumarin linked pyrazolinyl as urease inhibitors, kinetic mechanism and molecular docking, Chem. Biodivers. 14 (2017) e1700035.
[44] R.U. Kadam, N. Roy, Recent trends in drug-likeness prediction: a comprehensive review of in silico methods, Indian J Pharm Sci. 69 (2007) 609–615.
[45] M.A. Bakht, M.S. Yar, S.G. Abdel-Hamid, Molecular properties prediction, synthesis and antimicrobial activity of some newer oxadiazole derivatives, Eur. J. Med.

Chem. 45 (2010) 5862–5869.
[46] S. Tian, J. Wang, Y. Li, The application of in silico drug-likeness predictions in pharmaceutical research, Adv. Drug Deliv. Rev. 86 (2015) 2–10.
[47] W.P. Walters, M.A. Ajay, A.A. Murcko, Recognizing molecules with drug-like properties, Curr. Opin. Chem. Biol. 3 (1999) 384–387.
[48] A. Saeed, P.A. Mahesar, P.A. Channar, Q. Abbas, F.A. Larik, M. Hassan, H. Raza, S.Y. Seo, Synthesis, molecular docking studies of coumarinyl-pyrazolinyl substituted thiazoles as non-competitive inhibitors of mushroom tyrosinase, Bioorg. Chem. 74 (2017) 187–196.
[49] F.A. Larik, A. Saeed, P.A. Channar, U. Muqadar, Q. Abbas, M. Hassan, S.Y. Seo, M. Bolte, Design, synthesis, kinetic mechanism and molecular docking studies of novel 1-pentanoyl-3-arylthioureas as inhibitors of mushroom tyrosinase and free radical scavengers, Eur. J. Med. Chem. 141 (2017) 273–281.
[50] M. Hassan, Z. Ashraf, Q. Abbas, H. Raza, S.Y. Seo, Exploration of novel human tyrosinase inhibitors by molecular modelling, docking and simulation studies, Interdiscip. Sci. 10 (2018) 68–80.
[51] Q. Abbas, Z. Ashraf, M. Hassan, H. Nadeem, M. Latif, S. Afzal, S.Y. Seo, Development of highly potent melanogenesis inhibitor by in vitro, in vivo and computational studies, Drug Des. Dev. Therapy 11 (2017) 2029–2046.
[52] Q. Abbas, H. Raza, M. Hassan, A.R. Phull, S.J. Kim, S.Y. Seo, Acetazolamide inhibits the level of tyrosinase and melanin: an enzyme kinetic, in vitro, in vivo and in silico studies, Chem. Biodivers. 14 (2017) e1700117.
[53] A.R.S. Butt, M.A. Abbasi, S.Z. Siddiqui, H. Raza, M. Hassan, S.A. Ali Shah, M. Shahid, S.Y. Seo, Synthesis and structure-activity relationship of tyrosinase inhibiting novel bi-heterocyclic acetamides: mechanistic Insights through enzyme Inhibition, kinetics and computational studies, Bioorg. Chem. 86 (2019) 459–472.
[54] R.A. Friesner, R.B. Murphy, M.P. Repasky, L.L. Frye, J.R. Greenwood, T.A. Halgren, P.C. Sanschagrin, D.T. Mainz, Extra precision glide: docking and scoring incorporating a model of hydrophobic enclosure for protein-ligand complexes, J. Med. Chem. 49 (2006) 6177–6196.
[55] R. Farid, T. Day, R.A. Friesner, R.A. Pearlstein, New insights about HERG blockade obtained from protein modeling, potential energy mapping, and docking studies, Bioorg. Med. Chem. 14 (2006) 3160–3173.